

A Chemical–Biological Evaluation of Rhodium(I) *N*-Heterocyclic Carbene Complexes as Prospective Anticancer Drugs

Luciano Oehninger,^[a] Laura Nadine Küster,^[b] Claudia Schmidt,^[a]
Alvaro Muñoz-Castro,^[c] Aram Prokop,^[b] and Ingo Ott*^[a]

Abstract: Rhodium(I) complexes bearing *N*-heterocyclic carbene (NHC) ligands have been widely used in catalytic chemistry, but there are very few reports of biological properties of these organometallics. A series of Rh^I-NHC derivatives with 1,5-cyclooctadiene and CO as secondary ligands were synthesized, characterized, and biologically investigated as prospective antitumor drug candidates. Pronounced antiproliferative effects were noted for all com-

plexes, along with moderate inhibitory activity of thioredoxin reductase (TrxR) and efficient binding to biomolecules (DNA, albumin). Biodistribution studies showed that the presence of albumin lowered the cellular uptake

and confirmed the transport of rhodium into the nuclei. Changes in the mitochondrial membrane potential (MMP) were observed as well as DNA fragmentation in wild-type and daunorubicin- or vincristine-resistant Nalm-6 leukemia cells. Overall, these studies indicated that Rh^I-NHC fragments could be used as partial structures of new antitumor agents, in particular in those drugs designed to address resistant malignant tissues.

Keywords: antitumor agents • carbenes • cytotoxicity • drug resistance • rhodium • thioredoxin reductase

Introduction

Over the last years organometallic complexes have experienced an increasing interest not only because of their catalytic properties but also due to their fascinating biological effects.^[1–4] Among those, organometallics bearing *N*-heterocyclic carbenes (NHCs) as ligands have been increasingly in the focus of inorganic medicinal chemists.^[5–7] The advantages of NHC ligands include the fact that sufficiently stable coordinative bonds can be formed to many different metals and that the versatile synthetic chemistry related to the use of NHC ligands offers a broad variety of possible structural modifications. So far, metal-NHC complexes have been mostly studied as new antibacterial and anticancer agents. Although research on anti-infectives has been largely focused on Ag^I-NHC complexes,^[8–11] Au^I-NHC derivatives are the most studied examples concerning new anticancer

agents.^[12–15] This type of complex showed among other effects a strong and selective inhibition of the enzyme thioredoxin reductase (TrxR), induction of apoptosis, or depolarization of the mitochondrial membrane.^[14,16–19] Besides gold and silver, other metals including platinum,^[20–24] palladium,^[25,26] ruthenium,^[27–29] or rhodium^[30,31] have also been used as centers of bioactive NHC complexes.

Rhodium complexes have been widely studied as anticancer agents mainly containing Rh^{III} coordinated to different ligands such as polypyridyls or cyclopentadienyls (see Figure 1 for some selected examples).^[32–40] Biological studies on rhodium(I) complexes as anticancer agents are less frequent.^[31,41–44] One recent report by McAlpine and co-workers described the alteration of cell migration, DNA replication, and DNA condensation by a Rh^I-NHC derivative.^[31] The choice of Rh^I as metal center appears promising because it is isoelectronic with platinum(II) and exhibits a square-planar geometry like cisplatin-type tumor therapeutics.

In recent studies we and others reported on the promising anticancer effects of gold(I)- and ruthenium(II)-NHC complexes containing benzimidazol-2-ylidene ligands.^[14,16,28,30,45–48] Starting from this type of NHC ligand we designed in this study a series of related NHC ligands with different surface volumes, lipophilicities, and coordinative donor strengths (see Scheme 1). Perimidines have been described as DNA intercalating agents and therefore NHC ligands derived of this *N*-heterocyclic core were included in the study.^[49] The target Rh^I complexes contain the respective NHC moiety as well as chlorido, 1,5-cyclooctadiene (COD), or carbon monoxide (CO) ligands, which themselves exhibit different coordinative and physicochemical

[a] L. Oehninger, C. Schmidt, Prof. Dr. I. Ott
Institute of Medicinal and Pharmaceutical Chemistry
Technische Universität Braunschweig, Beethovenstrasse 55
38106 Braunschweig (Germany)
Fax: (+49) 531 391 8456
E-mail: ingo.ott@tu-bs.de

[b] L. N. Küster, Dr. med. habil. Dr. rer. nat. A. Prokop
Department of Paediatric Oncology, Childrens Hospital Cologne
Amsterdamer Strasse 59, 50735 Cologne (Germany)

[c] Prof. Dr. A. Muñoz-Castro
Department of Chemical Sciences
Universidad Andres Bello
Republica 275, Santiago (Chile)

Supporting information for this article is available on the WWW under <http://dx.doi.org/10.1002/chem.201302819>.

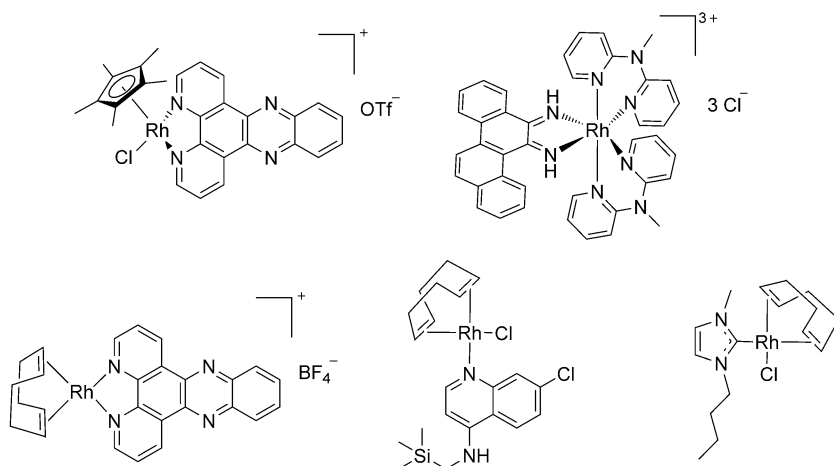
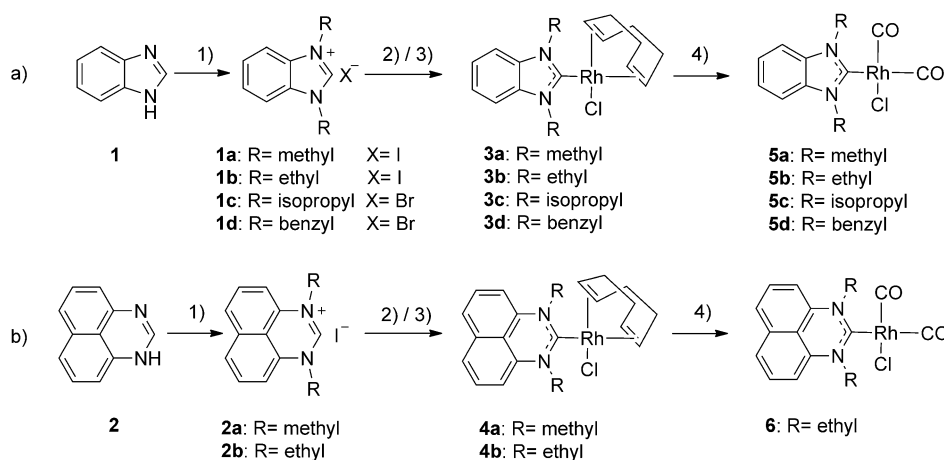


Figure 1. Examples of antitumor active rhodium complexes.



Scheme 1. Synthesis procedures: 1) alkyl halide, K_2CO_3 , CH_3CN , heat at reflux, 6 h; 2) Ag_2O in CH_2Cl_2 , 4 h; 3) $[RhCl(cod)]_2$, 2–12 h; 4) CO atmosphere in CH_2Cl_2 , 20 min.

properties and could hence be used to modulate the characteristics of the target complexes.

The synthesis and characterization of these Rh^I -NHC derivatives as well as their biological evaluation as prospective anticancer drugs are reported here. The antiproliferative effects of the complexes were evaluated, along with studies on possible molecular mechanisms of drug action (TrxR inhibition, DNA binding, effects on mitochondrial membrane potential) and effects in drug-resistant leukemia cells.

Results and Discussion

Synthesis and characterization: The complexes were prepared according to procedures depicted in Scheme 1. Complexes **3a–c** and **5b,c** have been described previously.^[50–53]

The benzimidazolium and perimidinium halides **1a–d** and **2a,b** were synthesized by heating benzimidazole or perimidine at reflux with an excess of an alkyl halide in the presence of K_2CO_3 . Next, compounds **1a–d** and **2a,b** were treated with a half equivalent of Ag_2O in CH_2Cl_2 to generate

a silver intermediate, followed by a transmetalation reaction by addition of bis[chlorido(1,5-cyclooctadiene)rhodium(I)] (see Scheme 1). The resulting benzimidazolylidene-rhodium(1,5-cyclooctadiene) derivatives (**3a–d**) and perimidinylidene-rhodium(1,5-cyclooctadiene) complexes (**4a** and **4b**) were purified by filtration over Celite and recrystallized from a mixture of CH_2Cl_2/n -hexane (1:4) at $0^\circ C$. In the case of **3a–d**, the reaction was complete within 4 h, whereas an extended reaction period of 24 h was required in the case of **4a** and **4b**. The dicarbonylrhodium(I) derivatives **5a–d** and **6** were obtained by stirring the respective $[Rh(cod)]$ complex in dichloromethane under carbon monoxide atmosphere for 20 min. The volume of the solution was reduced, n -hexane was added, and the solution was stored at $-20^\circ C$. After approximately 10 h the corresponding complexes had precipitated as pale-yellow solids. All target complexes were clearly characterized by MS and NMR spectroscopy (see below) and their high purity was confirmed by elemental analysis.

In the case of CO-containing complexes, IR spectroscopic analyses were also performed. In particular, the CO complexes were included in this study to compare the donor properties of the NHC ligands among each other by observing the IR band of the CO ligand ($\nu_{CO}(A_1)$).^[54,55] Ligands that are positioned trans to a CO ligand can have strong effect on the ability of the CO ligand to effectively π -backbond to the metal and this influences the IR-stretching frequencies of the CO ligand. Free CO shows a band at 2155 cm^{-1} ; a strong donating ligand will shift the CO band to lower frequencies.^[56] This shift was observed for all CO complexes but between the single complexes no strong variation could be noted in the $\nu_{CO}(A_1)$ bands, which were in the range of $2074\text{--}2086\text{ cm}^{-1}$. The 1,3-diisopropylbenzimidazolylidene ligand of **5c** had the weakest donor properties of the used NHC ligands with $\nu_{CO}(A_1)=2086\text{ cm}^{-1}$, whereas the methyl derivative **5a** had strongest one ($\nu_{CO}(A_1)=2074\text{ cm}^{-1}$). The $\nu_{CO}(A_1)$ bands of the N -ethyl complexes **5b** (2077 cm^{-1}) and **6** (2079 cm^{-1}) indicated that the σ -donation of the benzimidazolylidene- and perimidinylidene-NHC ligands was similar.

NMR spectroscopy: In the ^1H NMR spectra of the benzimidazolium and perimidinium halides, **1a,b** and **2a,b**, respectively (see Figure S1, the Supporting Information) the protons of the C^2 position in **1a,b** ($\delta=9.65$ and 9.80 ppm, respectively^[16]) are shifted to higher ppm values compared with those of **2a,b** ($\delta=9.01$ and 8.95 ppm, respectively). This difference is reflected in a higher acidity and hence reactivity of **1ab** with silver oxide and explains the longer reaction time necessary to obtain the $[\text{Rh}(\text{cod})(\text{perimidinylidene})]$ complexes (see above).

In the ^1H NMR spectra of the COD derivatives **3b** and **3d** the signal of the $\text{N}-\text{CH}_2-\text{R}$ protons is split into two signals (Figure 2, (a) signals), which is the consequence of an

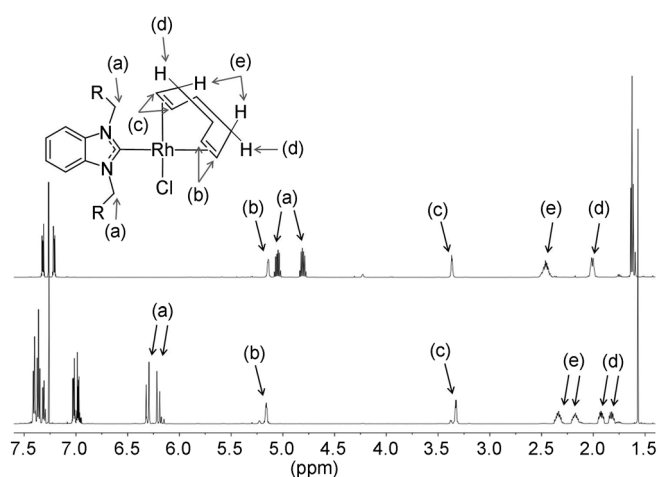


Figure 2. ^1H NMR spectra of **3b** (top) and **3d** (bottom) in CDCl_3 , $\text{N}-\text{CH}_2-\text{R}$ (a); *trans*-CH of COD (b); *cis*-CH of COD (c); equatorial- CH_2 of COD (d); axial- CH_2 COD (e).

asymmetrical disposition of the *N*-residues regarding the $[\text{Rh}(\text{cod})]$ moiety. The same effect was also observed for complex **4b**. However, in this case the $\text{N}-\text{CH}_2-\text{R}$ signals were not well-defined and appeared as broad multiplets. Of note, similar phenomena can also be observed with Ru^{II} -NHC derivatives.^[28]

The $[\text{RhCl}(\text{cod})]$ moiety shows a characteristic pattern in the ^1H NMR spectrum, in which two signals are observed that correspond to the *cis*- and *trans*-olefin protons regarding the NHC ligand (signals (c) and (b) in Figure 2, respectively), as well as two signals from the equatorial and axial CH_2 protons (signals (d) and (e) in Figure 2, respectively). This signal distribution was corroborated by an exemplary 2D NMR spectrum of **3a** (see Figure S2, the Supporting Information).

In complex **3d** the equatorial and axial proton signals become unfolded due to the steric influence of the benzyl residues of the NHC moiety over the COD ligand (see Figure 2, bottom, signals (d) and (e)).

The olefinic CH groups *cis* and *trans* to the NHC ligands show Rh–C coupling constants in the ^{13}C NMR spectra of **3a–d** and **4a,b**. The NHC moiety has a stronger *trans* effect in comparison to the chlorido ligand and the resulting rela-

tive labilization of the coordinative bond between Rh and the respective *trans*-positioned alkene fragment is reflected in smaller coupling constants (*trans* to NHC: $^1J_{\text{RhC}}=6.6\text{--}6.8$ Hz, *cis* to NHC: $14.2\text{--}14.6$ Hz).^[57]

Exchange of the COD with two CO ligands caused an up-field shift of the C^2 signals of around $\delta=11\text{--}12$ ppm in the ^{13}C NMR spectra. This indicates a weaker influence of the rhodium atom over the C^2 carbon of the NHC ligand in the CO derivatives compared with the COD complexes. An increase in the NHC–Rh distance can be assumed by comparing the coupling constants between the NHC– C^2 carbon and Rh (e.g., $J=51$ Hz for **3b** and 43 Hz for **5b**, respectively). In the ^{13}C NMR spectra of the perimidinylidene derivative **6**, the NHC– C^2 is shifted to lower ppm values compared with the benzimidazolylidene complexes **5a,b**. Taken together, the signals for the *cis*- ($^1J_{\text{RhC}}\approx 74$ Hz) and *trans*- ($^1J_{\text{RhC}}\approx 55$ Hz) CO ligands can also be distinguished in the ^{13}C NMR spectra according to their coupling constants (see Figure 3).

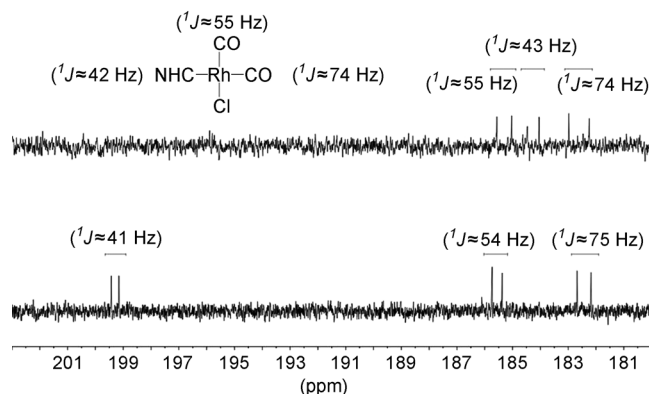


Figure 3. Rh–C couplings in ^{13}C NMR spectra (CDCl_3) of **5b** (top) and **6** (bottom).

Theoretical calculations: The geometry, bonding, and molecular properties of the studied compounds have been analyzed through relativistic density functional calculations. The COD moiety exhibits a nearly η^2, η^2 coordination mode, in which the Rh–COD bond lengths *trans* to the NHC ligand are slightly elongated (≈ 0.1 Å) in relation to the other Rh–COD distances (Table S1 and Figure S3, the Supporting Information). This is in good agreement with the results of the ^1H NMR measurements (see above). Similarly, the Rh–CO distances in the dicarbonyl counterparts are different, but to a small extent of about 0.64 Å. The Rh–NHC and Rh–Cl distances are similar within the studied series, displaying an averaged value of (2.07 ± 0.05) and (2.40 ± 0.02) Å, respectively, which are in the range of other similar compounds.^[58] Moreover, calculated ^{13}C NMR spectroscopy and ν_{CO} are in good agreement with the available experimental data (see the Supporting Information).

The calculated bond-dissociation energies (BDE) of the NHC–Rh bond display quite similar values for the studied series (Table S2, the Supporting Information), denoting a more stabilizing situation in the dicarbonyl counterparts

(av: 60.18 kcal mol⁻¹) in relation to the COD derivatives (av: 51.38 kcal mol⁻¹). A deeper understanding into the terms that contribute to the BDE in the framework of Morokuma–Ziegler energy decomposition analysis^[59] reveals that the main difference is attributable to the term that accounts for Pauli (steric) repulsion, which is more destabilizing in the COD derivatives (av: 17 kcal mol⁻¹) due to the shorter NHC–Rh distance (Table S1, the Supporting Information). In contrast, the term that accounts for the stabilizing covalent character of the NHC–Rh interaction due to the formation of bonds (sharing of electrons) is more favorable in this series (about of av. -4 kcal mol⁻¹) supporting the observations made by ¹³C NMR spectroscopy (see above).

The COD ligand exhibits a BDE of about 88.03 kcal mol⁻¹, and the CO ligand exhibits values of 38.68 kcal mol⁻¹ (*trans* to the NHC moiety) and 57.03 kcal mol⁻¹ (*cis*). In contrast, the chlorido ligand exhibits a higher BDE (≈124 kcal mol⁻¹ for COD derivatives, and ≈145 kcal mol⁻¹ for the dicarbonyl counterparts, however, denoting a more polarized situation that prompts its abstraction in polar solvents. Thus, the differences observed for the chemical behavior of systems involving the methyl- and benzyl side chains, namely, compounds **3a**, **5a** and **3d**, **5d**, concerning their behavior in the biochemical assays (see below) and in solution (DMF and H₂O), are ascribed to steric-hindrance effects, which hinder the access towards the rhodium center for external groups or molecules. Lastly, we evaluate the rotation of the benzyl group (Figure 4), which seems to protect the metallic center from solvent molecules, in relation to the methylated-NHC ligand of **3a**.

Biological screening as antiproliferative agents and TrxR inhibitors: Motivated by previous results on metal-NHC complexes the initial biological screening as prospective anticancer drugs consisted of measuring the cell growth inhibitory activities in cultured cancer cells as well as the inhibitory effects against the enzyme TrxR.^[12,14–18,28,60]

The triggering of antiproliferative effects by the rhodium(I) derivatives was investigated in two tumor cell lines (namely, MCF-7 human breast adenocarcinoma and HT-29 colon carcinoma). The rhodium-free cations **1a** and **2a**, as

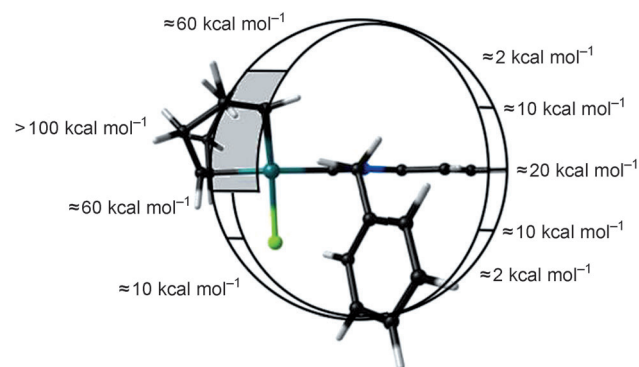


Figure 4. Qualitative energy barrier for the rotation of the benzyl group in **3d** (half of the NHC ligand has been removed for clarity).

well as the dirhodium Rh^I synthesis reagent bis[chlorido(1,5-cyclooctadiene)rhodium(I)] ([RhCl(cod)]₂) were inactive (IC₅₀ values > 100 μM, see Table 1). In contrast, all [Rh(cod)-

Table 1. IC₅₀ values of antiproliferative effects in MCF-7 and HT-29 cells and inhibition of TrxR; the results are expressed as means (± error) of repeated experiments.

Complex	IC ₅₀ [μM]		
	MCF-7	HT-29	TrxR
1a	> 100	> 100	> 100
[RhCl(cod)] ₂	> 100	> 100	n.d.
2a	> 100	> 100	> 100
3a	0.6 ± 0.2	0.9 ± 0.0	1.8 ± 0.2
3b	2.9 ± 0.8	4.2 ± 0.5	1.5 ± 0.1
3c	2.2 ± 1.3	2.9 ± 0.7	1.5 ± 0.4
3d	2.3 ± 0.3	2.7 ± 0.1	2.0 ± 0.2
4a	2.4 ± 0.6	6.6 ± 1.3	1.7 ± 0.3
4b	3.0 ± 0.8	5.6 ± 0.7	1.9 ± 0.1
5a ^[a]	7.6 ± 0.1	10.2 ± 2.3	n.d.
5b ^[a]	5.0 ± 2.3	10.8 ± 3.5	n.d.
5c	> 100	97.2 ± 0.6	2.3 ± 0.4
5d	47.5 ± 4.0	43.6 ± 1.4	1.2 ± 0.3

[a] Obvious decomposition during the assay procedure. n.d.: not determined.

(NHC)] derivatives (**3a–d** and **4ab**) were active at low micromolar concentrations against both cancer cell lines with IC₅₀ values in the 0.6–3.0 μM range in MCF-7 cells and in the 0.9–6.6 μM range in HT-29 cells. The most active [Rh(cod)] complex was **3a**, which triggered IC₅₀ values below 1.0 μM in both cell lines. Compound **6** experienced solubility problems under the assay conditions and was not studied further. Whereas the carbonyl complexes **5a** and **5b** showed antiproliferative effects in the low micromolar range (IC₅₀ = 5–11 μM), complexes **5d** and **5c** were low-active or inactive (IC₅₀ values > 40 μM). However, for solutions of complexes **5a,b** a color change and the formation of a precipitate from the aqueous solution was noted during the first hour of incubation. This clearly indicated the formation of decomposition products that might have influenced the outcome of the biological tests. The color change was not observed for complexes **5c,d** and their aqueous solutions remained visually unchanged for 12 h. Based on these observations complexes **5a,b** were excluded from further biological tests.

Next, the ability to inhibit TrxR was investigated. The rhodium-free ligands **1a** and **2a** expectedly showed no activity up to 100 μM. For the investigated NHC complexes **3a–d**, **4a,b** and **5c,d**, IC₅₀ values were observed in a narrow range around 1.5 μM. Hence the activity against TrxR was largely independent on the NHC ligand structure and can be considered as moderate compared with other metal-NHC complexes investigated in exactly the same assay.^[14,16,17,28]

Binding to biomolecules, cellular distribution, and effects in resistant cell lines of 3a: For further extended studies, complex **3a** was selected as the strongest antiproliferative agent. Metal complexes, including NHC derivatives, are known to interact with and bind to several biomolecules such as albumin or DNA. Binding of **3a** to albumin and DNA was pre-

liminarily evaluated by precipitation assays and quantification of rhodium by atomic absorption spectroscopy (see the Experimental Section for details).

After 2 h of exposure to albumin, (67 ± 10)% of the total rhodium was bound to albumin and the values remained rather stable over an extended exposure up to 24 h. Complexes **3b** and **3c** were used for comparison and showed a very similar behavior (see the Supporting Information for more details). Next, DNA was exposed to **3a** as well as the platinum anticancer drug cisplatin (as a reference) at a nucleotide/metal ratio of 200:1 for 4 h and the percentage of the total amount of metal attached to DNA was determined. Under these conditions (72 ± 3)% of rhodium of **3a** was bound to the DNA, whereas DNA platination caused by cisplatin was (26 ± 3)%. The efficient binding to DNA is in good agreement with the recent results by McAlpine et al.^[31] Overall, these experiments clearly indicate that Rh^I -NHC complexes can undergo strong molecular interactions with relevant biomolecules. To understand the relevance of these interactions in a more complex system, the uptake of **3a** in whole HT-29 cells and into their nuclei was determined. The cellular uptake was measured in a comparative manner from the serum-free cell culture medium and from the same medium with added albumin. This experimental setup enables the evaluation of the influence of albumin on rhodium bioavailability. The experiments were performed with a concentration of **3a** of $1.0 \mu\text{M}$, which is related to the IC_{50} value of the complex in this cell line. As observed in Figure 5 a, the level of cellular rhodium was higher in the experiments with albumin-free medium than in those containing albumin. This indicated that the presence of serum albumin has a negative influence on the uptake process of **3a**.

For the evaluation of the rhodium uptake into the nuclei of HT-29 cells, the experimental setup was changed to reflect the standard cell culture conditions under which **3a** would trigger strong cytotoxic effects (experiments with **3a** ($5.0 \mu\text{M}$) in serum containing cell culture medium, see Figure 5 b). In these experiments, well-detectable rhodium levels were reached that were higher after short exposure (1 h) than after longer incubation (6 h). However, these amounts corresponded to only 1–2% of the total cellular rhodium.

The cytotoxic action and apoptosis induction of many anticancer drugs is related to changes in the mitochondrial membrane potential (MMP). For **3a**, moderate MMP changes in Nalm-6 leukemia cells were observed at concentrations between 0.25 and $1.5 \mu\text{M}$ ($<40\%$), whereas drastically increased effects ($>80\%$) were noted at a concentration of $2.0 \mu\text{M}$ (see Figure 6a).

The DNA fragmentation by **3a** as a parameter of apoptosis induction was assessed in wild-type- as well as in daunorubicin- or vincristine-resistant P-glycoprotein (P-gp) overexpressing Nalm-6 cells.^[16] A strong DNA fragmentation was observed in all Nalm-6 cell lines in concentrations higher than $0.5 \mu\text{M}$. In concentrations of $0.75 \mu\text{M}$ (in daunorubicin-resistant cells) or $1.0 \mu\text{M}$ (in vincristine-resistant cells) and higher, drug resistance could be clearly overcome as evi-

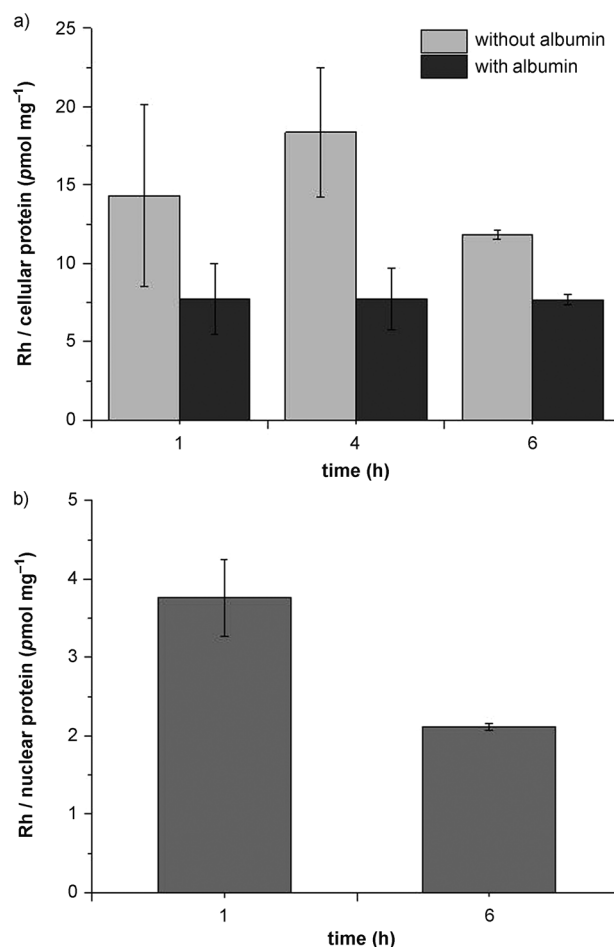


Figure 5. a) Cellular uptake of **3a** ($1.0 \mu\text{M}$) from cell culture media with and without albumin into HT-29 cells; b) Rhodium levels in nuclei exposed to of **3a** ($5.0 \mu\text{M}$).

denced by at least 40% apoptotic cells. Accordingly, the calculated IC_{50} values from these experiments were comparable (Nalm-6: (0.6 ± 0.1) μM , Nalm-6-DNR: (0.6 ± 0.1) μM , Nalm-6-VCR: (1.0 ± 0.1) μM).

Conclusion

Rh^I -NHC complexes with COD or CO secondary ligands were prepared and characterized. Both spectroscopic and theoretical evaluations indicated a higher kinetic stability of the COD complexes compared with the dicarbonyl analogues. This was further confirmed when the complexes were subjected to biological screening as some of the CO complexes experienced major stability problems in biological media. Further limitations for biological applications were related to insufficient solubility in aqueous environment, especially in the case of the larger perimidine-derived NHC ligands.

However, complexes of the general structure $[Rh^I Cl(benzimidazolylidene)(cod)]$ did not experience the mentioned problems, showed pronounced antiproliferative

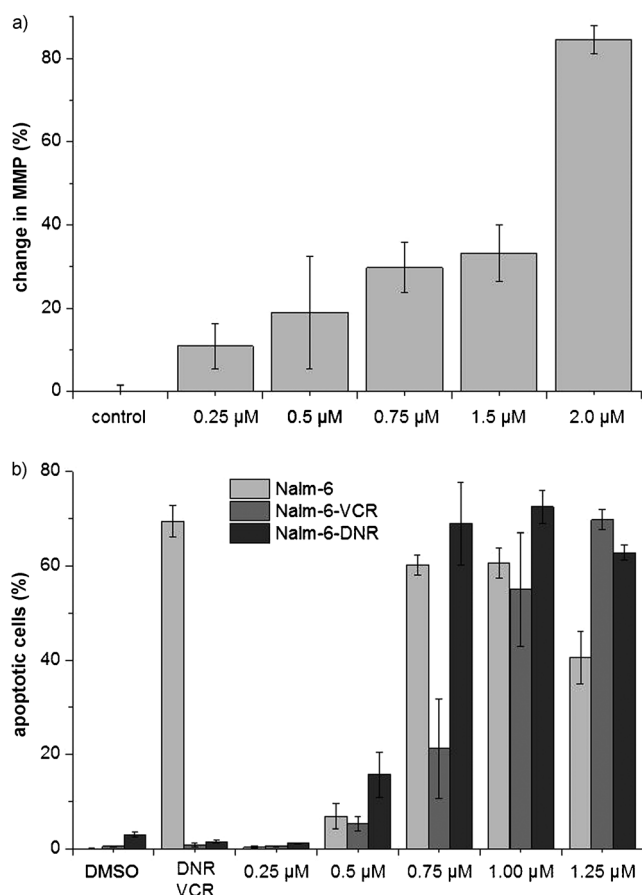


Figure 6. a) Changes in the mitochondrial membrane potential of Nalm-6 cells after 48 h incubation with **3a**; b) Apoptosis induction determined as nuclear DNA fragmentation after 72 h drug exposure in wild-type Nalm-6 cells as well as daunorubicin- (Nalm-6-DNR) or vincristine-resistant (Nalm-6-VCR) subtypes. Values are given as percentages of cells with hypodiploid DNA (\pm SD ($n=3$)). Resistance to daunorubicin (DNR) and vincristine (VCR) was confirmed by the missing or very low apoptosis induction after exposure to DNR (52.5 nM) or VCR (20 nM).

effects in cultured tumor cells, and were moderate inhibitors of TrxR. TrxR is an enzyme that is involved in several disease-relevant pathways and has to be considered as a possible molecular target for various metallodrugs.^[61–68] Taken together, this also suggests TrxR inhibition as a relevant contributing factor in the chemical biology of $[\text{Rh}^{\text{I}}\text{Cl}(\text{cod})\text{-(NHC)}]$ metallodrugs, although it is unlikely their major mode of action.

Because the rhodium-free cationic ligand precursors and rhodium(I) in the form of $[\text{RhCl}(\text{cod})]_2$ were devoid of any activity in the biological assays, it can be speculated that the $[\text{Rh}^{\text{I}}(\text{benzimidazolylidene})]$ fragment represents a useful vehicle to deliver Rh^{I} to biological tissues.

More detailed studies on the most active derivative **3a** showed effective binding to albumin and DNA. Albumin contains an accessible cysteine residue (Cys-34) as most probable binding site for metal species, whereas binding to DNA was not unexpected based on the similar chemical features of Rh^{I} and platinum(II) (isoelectronic, square-planar geometry).

Total cellular-uptake studies showed that the presence of albumin lowered the rhodium uptake. Rhodium was well-detectable in isolated nuclei, however, at a low percentage of the total. The relevance of the nuclear rhodium uptake is not clear at this stage. On the one hand, the absolute values are low compared with that of other metallodrugs investigated under similar experimental conditions, on the other hand, DNA targeting by the drug cisplatin also leads to a small extent of DNA platination and the low relative uptake of metals into nuclei is common.^[69–72]

Complex **3a** also triggered considerable changes in the mitochondrial membrane potential and led to DNA fragmentation, which underline the potential of this metallodrug as a cytotoxic and apoptosis-inducing agent. Moreover, complex **3a** effectively overcame P-gp-related drug resistance to daunorubicin and vincristine in leukemia cells, a property highly desirable in the design of prospective anti-cancer drugs.

In consequence, $[\text{Rh}^{\text{I}}\text{Cl}(\text{benzimidazolylidene})(\text{cod})]$ complexes showed promising properties for the design of new cancer chemotherapeutics. Further exploration of this type of bioorganometallics is highly warranted and is the subject of ongoing studies.

Experimental Section

General: All reagents and the solvents were used as received from Sigma, Aldrich, or Fluka. ^1H NMR spectra were recorded on a Bruker DRX-400 AS NMR spectrometer and ^{13}C NMR spectra on a Bruker AV II-600 AS NMR spectrometer, MS spectra were recorded on a Finnigan MAT4515. The purity of the target compounds was confirmed by elemental analysis (Flash EA112, Thermo Quest Italia). For all compounds undergoing biological evaluation, the experimental values differed less than 0.5% from the calculated ones. Perimidine and the benzimidazolium salts **1a–d** were synthesized as described in the literature.^[16,49] Cell culture: MCF-7 breast adenocarcinoma and HT-29 colon carcinoma cells were maintained in DMEM high glucose (PAA) supplemented with 50 mg L⁻¹ gentamycin and 10% (v/v) fetal calf serum (FCS) prior to use. Nalm-6 leukemia cells were maintained in RPMI medium supplemented with 1% penicillin/streptomycin and 10% (v/v) FCS.

Synthesis of perimidine (2):^[49] 1,8-Diaminonaphthalene (1.140 g, 7.0 mmol) was dissolved in ethanol (20 mL), followed by addition of an excess of formic acid (1.60 mL, 40 mmol). The mixture was heated at reflux for 4 h under nitrogen atmosphere. The ethanolic solution was diluted with water and neutralized by addition of NH_4OH at 0°C. The precipitate was collected and washed 4 times with water and dried at 50°C for 12 h. Yield: 1.119 g (6.7 mmol, 95%) light-brown powder. ^1H NMR (CDCl_3): δ = 3.24 (brs, 1H, NH), 6.47 (d, 2H, $J_{\text{HH}} = 6.8$ Hz, $\text{ArH}_{4/9}$), 7.11 (m, 4H, ArH_{5-8}), 7.23 ppm (s, 1H, ArH^2); elemental analysis calcd (%) for $\text{C}_{11}\text{H}_8\text{N}_2$: C 78.55, H 4.79, N 16.66; found: C 78.58, H 4.69, N 16.30.

General procedure for synthesis of the dialkylperimidinium halides: Perimidine (**2**) (1.009 g, 6 mmol), K_2CO_3 (1.037 g, 7.5 mmol) and an excess of the respective alkyl halide (18 mmol) were heated at reflux in acetonitrile for 8–14 h. The solvent was removed under reduced pressure and the resultant solid was resuspended in dichloromethane and filtered off to remove the formed potassium halide along with the remaining K_2CO_3 . The solvent of the filtrate was removed under reduced pressure and resuspended in tetrahydrofuran to remove the excess of alkyl halide and remaining perimidine. The obtained white solid corresponds to the pure desired product.

1,3-Dimethylperimidinium iodide (2a): Yield: 0.622 g (1.9 mmol, 32%) light-brown powder. $^1\text{H NMR}$ ($[\text{D}_6]\text{DMSO}$): δ = 3.52 (s, 6H, $-\text{NCH}_3$), 7.04 (d, 2H, ArH, $^3J_{\text{HH}} = 7.6$ Hz), 7.54 (dd, 2H, ArH, $^3J_{\text{HH}} = 7.6$ Hz, $^3J_{\text{HH}} = 8.4$ Hz), 7.65 (d, 2H, ArH, $^3J_{\text{HH}} = 8.4$ Hz), 9.01 ppm (s, 1H, ArH 2); $^{13}\text{C NMR}$ ($[\text{D}_6]\text{DMSO}$): δ = 38.67 ($-\text{NCH}_3$), 107.64 (ArC), 120.35 (quaternary ArC), 123.53 and 128.36 (ArC), 132.84 and 133.84 (quaternary ArC), 153.32 ppm (ArC 2); elemental analysis calcd (%) for $\text{C}_{13}\text{H}_{13}\text{N}_2\text{I}$: C 48.17, H 4.04, N 8.64; found: C 47.98, H 4.31, N 8.50.

1,3-Diethylperimidinium iodide (2b): Yield: 0.622 g (1.9 mmol, 32%) light-brown powder. $^1\text{H NMR}$ ($[\text{D}_6]\text{DMSO}$): δ = 1.41 (t, 6H, $-\text{NCH}_2\text{CH}_3$, $^3J_{\text{HH}} = 7.1$ Hz), 4.03 (q, 4H, $-\text{NCH}_2\text{CH}_3$, $^3J_{\text{HH}} = 7.1$ Hz), 7.12 (d, 2H, ArH, $^3J_{\text{HH}} = 7.7$ Hz), 7.52 (dd, 2H, ArH, $^3J_{\text{HH}} = 7.7$ Hz, $^3J_{\text{HH}} = 8.3$ Hz), 7.62 (d, 2H, ArH, $^3J_{\text{HH}} = 8.3$ Hz), 8.95 ppm (s, 1H, ArH 2); $^{13}\text{C NMR}$ ($[\text{D}_6]\text{DMSO}$): δ = 11.82 ($-\text{NCH}_2\text{CH}_3$), 46.72 ($-\text{NCH}_2\text{CH}_3$), 107.65 (ArC), 121.13 (quaternary ArC), 123.39 and 128.31 (ArC), 131.43 and 134.43 (quaternary ArC), 152.36 ppm (s, ArC 2); elemental analysis calcd (%) for $\text{C}_{15}\text{H}_{17}\text{N}_2\text{I}$: C 51.15, H 4.86, N 7.95; found: C 51.08, H 4.49, N 7.55.

General procedure for synthesis of the [Rh(cod)(NHC)] derivatives: The respective benzimidazolium- or perimidinium halide (0.32 mmol) and Ag_2O (0.0371 g, 0.16 mmol) were added to a dried Schlenk tube. The mixture was backflashed three times with N_2 and then dry CH_2Cl_2 was added (15 mL). The flask was closed and stirred for 4 h in the dark. A solution of bis[chlorido(η^2,η^2 -cycloocta-1,5-diene)rhodium(I)] (0.078 g, 0.16 mmol) in CH_2Cl_2 was added (10 mL) and the solution was stirred for 2–12 h in the dark. The obtained suspension was filtered over Celite (281 nm) and concentrated in a vacuum. The yellow residue was recrystallized from $\text{CH}_2\text{Cl}_2/n$ -hexane (10/40 mL) at 4°C.

Chlorido(η^2,η^2 -cycloocta-1,5-diene)(1,3-dimethylbenzimidazol-2-ylidene)rhodium(I) (3a): The preparation of this compound has been reported previously.^[50] Yield: 0.084 g (0.21 mmol, 69%) yellow powder. $^1\text{H NMR}$ (CDCl_3): δ = 2.01–2.12 (m, 4H, CH_2 COD), 2.44–2.57 (m, 4H, CH_2 COD), 3.40 (m, 2H, CH COD), 4.35 (s, 6H, $-\text{NCH}_3$), 5.20 (m, 2H, CH COD), 7.23 (m, 2H, ArH $_{4/7}$), 7.28 ppm (m, 2H, ArH $_{5/6}$); $^{13}\text{C NMR}$ (CDCl_3): δ = 28.85 (CH_2 COD), 32.97 (CH_2 COD), 34.64 ($-\text{NCH}_3$), 68.35 (d, *cis*-CH COD, $^1J_{\text{RhC}} = 14.9$ Hz), 100.35 (d, *trans*-CH COD, $^1J_{\text{RhC}} = 6.8$ Hz), 109.25 and 122.38 ppm (ArC), 135.32 (quaternary ArC), 196.14 ppm (d, ArC 2 , $^1J_{\text{RhC}} = 50.6$ Hz); MS (EI): m/z : 392 [M^+]; elemental analysis calcd (%) for $\text{C}_{17}\text{H}_{22}\text{N}_2\text{Cl}_2\text{Rh}$: C 51.99, H 5.65, N 7.13; found: C 51.68, H 5.59, N 6.97.

Chlorido(η^2,η^2 -cycloocta-1,5-diene)(1,3-diethylbenzimidazol-2-ylidene)rhodium(I) (3b): The preparation of this compound has been reported previously.^[16] Yield: 0.107 g (0.22 mmol, 72%) yellow powder. $^1\text{H NMR}$ (CDCl_3): δ = 1.63 (t, 6H, $-\text{NCH}_2\text{CH}_3$, $^3J_{\text{HH}} = 7.3$ Hz), 1.96–2.06 (m, 4H, CH_2 COD), 3.41–3.51 (m, 4H, CH_2 COD), 3.37 (m, 2H, CH COD), 4.81 (dq, 2H, $-\text{NCH}_2\text{CH}_3$, $^3J_{\text{HH}} = 7.3$ Hz, $^2J_{\text{HH}} = 14.4$ Hz), 5.05 (dq, 2H, $-\text{NCH}_2\text{CH}_3$, $^3J_{\text{HH}} = 7.3$ Hz, $^2J_{\text{HH}} = 14.4$ Hz), 5.14 (m, 2H, CH COD), 7.21 (dd, 2H, ArH $_{4/7}$, $^4J_{\text{HH}} = 3.1$ Hz, $^3J_{\text{HH}} = 6.0$ Hz), 7.32 ppm (dd, 2H, ArH $_{5/6}$, $^4J_{\text{HH}} = 3.1$ Hz, $^3J_{\text{HH}} = 6.0$ Hz); $^{13}\text{C NMR}$ (CDCl_3): δ = 14.96 ($-\text{NCH}_2\text{CH}_3$), 28.79 (CH_2 COD), 32.90 (CH_2 COD), 43.60 ($-\text{NCH}_2\text{CH}_3$), 68.58 (d, *cis*-CH COD, $^1J_{\text{RhC}} = 14.2$ Hz), 99.93 (d, *trans*-CH COD, $^1J_{\text{RhC}} = 6.7$ Hz), 109.88 and 122.11 (ArC), 134.44 (quaternary ArC), 195.23 ppm (d, ArC 2 , $^1J_{\text{RhC}} = 50.6$ Hz); MS (EI): m/z : 420 [M^+]; elemental analysis calcd (%) for $\text{C}_{19}\text{H}_{26}\text{N}_2\text{Cl}_2\text{Rh}$: C 52.50, H 5.87, N 5.83; found: C 52.64, H 5.72, N 5.65.

Chlorido(η^2,η^2 -cycloocta-1,5-diene)(1,3-diisopropylbenzimidazol-2-ylidene)rhodium(I) (3c): The preparation of this compound has been reported previously.^[53] Yield: 0.087 g (0.17 mmol, 55%) yellow powder. $^1\text{H NMR}$ (CDCl_3): δ = 1.70 (d, 6H, $-\text{NCH}(\text{CH}_3)_2$, $^3J_{\text{HH}} = 7.1$ Hz), 1.79 (d, 6H, $-\text{NCH}(\text{CH}_3)_2$, $^3J_{\text{HH}} = 7.1$ Hz), 1.94–2.04 (m, 4H, CH_2 COD), 2.39–2.49 (m, 4H, CH_2 COD), 3.46 (m, 2H, CH COD), 5.10 (m, 2H, CH COD), 6.49 (hept, 2H, $-\text{NCH}(\text{CH}_3)_2$, $^3J_{\text{HH}} = 7.1$ Hz), 7.14 (dd, 2H, ArH $_{4/7}$, $^4J_{\text{HH}} = 3.1$ Hz, $^3J_{\text{HH}} = 6.1$ Hz), 7.50 ppm (dd, 2H, ArH $_{5/6}$, $^4J_{\text{HH}} = 3.1$ Hz, $^3J_{\text{HH}} = 6.1$ Hz); $^{13}\text{C NMR}$ (CDCl_3): δ = 20.88 and 21.88 ($-\text{NCH}(\text{CH}_3)_2$), 28.76 (CH_2 COD), 32.88 (CH_2 COD), 53.87 ($-\text{NCH}(\text{CH}_3)_2$), 67.81 (d, *cis*-CH COD, $^1J_{\text{RhC}} = 14.5$ Hz), 99.17 (d, *trans*-CH COD, $^1J_{\text{RhC}} = 6.7$ Hz), 112.08 and 121.51 (ArC), 133.64 (quaternary ArC), 194.00 ppm (d, ArC 2 , $^1J_{\text{RhC}} = 50.3$ Hz); MS (EI): m/z : 448 [M^+]; elemental analysis calcd (%) for $\text{C}_{21}\text{H}_{30}\text{N}_2\text{Cl}_2\text{Rh}$: C 54.33, H 6.34, N 5.51; found: C 54.14, H 6.33, N 5.23.

(1,3-Dibenzylbenzimidazol-2-ylidene)chlorido(η^2,η^2 -cycloocta-1,5-diene)rhodium(I) (3d): Yield: 0.070 g (0.12 mmol, 35%) yellow powder. $^1\text{H NMR}$ (CDCl_3): δ = 1.76–1.87 (m, 2H, CH_2 COD), 1.87–1.98 (m, 2H, CH_2 COD), 2.06–2.24 (m, 2H, CH_2 COD), 2.26–2.41 (m, 2H, CH_2 COD), 3.25–3.43 (m, 2H, CH COD), 5.10–5.26 (m, 2H, CH COD), 6.20 (d, 2H, $-\text{NCH}_2\text{Ar}$, $^2J_{\text{HH}} = 15.8$ Hz), 6.31 (d, 2H, $-\text{NCH}_2\text{Ar}$, $^2J_{\text{HH}} = 15.8$ Hz), 6.98 (m, 2H, ArH $_{4/7}$, $^4J_{\text{HH}} = 3.0$ Hz, $^3J_{\text{HH}} = 6.3$ Hz), 7.02 (dd, 2H, ArH $_{5/6}$, $^4J_{\text{HH}} = 3.3$ Hz, $^3J_{\text{HH}} = 5.9$ Hz), 7.29–7.33 (m, 2H, $-\text{NCH}_2\text{ArH}$), 7.34–7.38 (m, 4H, $-\text{NCH}_2\text{ArH}$), 7.38–7.42 ppm (m, 4H, $-\text{NCH}_2\text{ArH}$); $^{13}\text{C NMR}$ (CDCl_3): δ = 28.65 (CH_2 COD), 32.74 (CH_2 COD), 52.96 ($-\text{NCH}_2\text{Ar}$), 69.19 (d, *cis*-CH COD, $^1J_{\text{RhC}} = 14.3$ Hz), 100.53 (d, *trans*-CH COD, $^1J_{\text{RhC}} = 6.6$ Hz), 110.93, 122.48, 127.08, 127.82, 128.90, 135.01, 136.15 (18C, ArC), 197.83 ppm (d, ArC 2 , $^1J_{\text{RhC}} = 51.0$ Hz); MS(EI): 544 [M^+]; elemental analysis calcd (%) for $\text{C}_{29}\text{H}_{30}\text{N}_2\text{Cl}_2\text{Rh}$: C 63.92, H 5.55, N 5.14; found: C 64.14, H 5.78, N 5.26.

Chlorido(η^2,η^2 -cycloocta-1,5-diene)(1,3-dimethylperimidin-2-ylidene)rhodium(I) (4a): Yield: 0.084 g (0.19 mmol, 61%) yellow powder. $^1\text{H NMR}$ (CDCl_3): δ = 1.94–2.04 (m, 4H, CH_2 COD), 2.44–2.48 (m, 4H, CH_2 COD), 3.40 (m, 2H, CH COD), 4.54 (s, 6H, $-\text{NCH}_3$), 5.08 (m, 2H, CH COD), 6.67 (m, 2H, ArH), 7.30–7.40 ppm (m, 4H, ArH); $^{13}\text{C NMR}$ (CDCl_3): δ = 28.86 (CH_2 COD), 32.52 (CH_2 COD), 43.16 ($-\text{NCH}_3$), 70.06 (d, *cis*-CH COD, $^1J_{\text{RhC}} = 14.6$ Hz), 98.22 (d, *trans*-CH COD, $^1J_{\text{RhC}} = 6.8$ Hz), 104.35 (ArC), 119.71 (quaternary ArC), 121.04 and 127.76 (ArC), 134.17 and 134.96 (quaternary ArC), 211.63 ppm (d, ArC 2 , $^1J_{\text{RhC}} = 48.6$ Hz); MS(EI): m/z : 442 [M^+]; elemental analysis calcd (%) for $\text{C}_{21}\text{H}_{24}\text{N}_2\text{Cl}_2\text{Rh}$: C 51.99, H 5.65, N 7.13; found: C 51.68, H 5.59, N 6.97.

Chlorido(η^2,η^2 -cycloocta-1,5-diene)(1,3-diethylperimidin-2-ylidene)rhodium(I) (4b): Yield: 0.072 g (0.15 mmol, 48%) brown powder. $^1\text{H NMR}$ (CDCl_3): δ = 1.59 (t, 6H, $-\text{NCH}_2\text{CH}_3$, $^3J_{\text{HH}} = 7.0$ Hz), 1.86–2.10 (m, 4H, CH_2 COD), 2.33–2.57 (m, 4H, CH_2 COD), 3.32 (m, 2H, CH COD), 4.68 (m, 2H, $-\text{NCH}_2\text{CH}_3$), 5.06 (m, 2H, CH COD), 6.29 (m, 2H, $-\text{NCH}_2\text{CH}_3$), 6.67 (dd, 2H, ArH, $^4J_{\text{HH}} = 1.2$ Hz, $^3J_{\text{HH}} = 7.3$ Hz), 7.27–7.35 ppm (m, 4H, ArH); $^{13}\text{C NMR}$ (CDCl_3): δ = 11.59 ($-\text{NCH}_2\text{CH}_3$), 28.85 (CH_2 COD), 32.51 (CH_2 COD), 49.96 ($-\text{NCH}_2\text{CH}_3$), 70.47 (d, *cis*-CH COD, $^1J_{\text{RhC}} = 14.6$ Hz), 97.73 (d, *trans*-CH COD, $^1J_{\text{RhC}} = 6.8$ Hz), 105.11 (ArC), 120.75 (quaternary ArC), 120.94 and 127.63 (ArC), 133.25 and 134.85 (quaternary ArC), 211.65 ppm (d, ArC 2 , $^1J_{\text{RhC}} = 48.5$ Hz); MS(EI): m/z : 470 [M^+]; elemental analysis calcd (%) for $\text{C}_{23}\text{H}_{28}\text{N}_2\text{Cl}_2\text{Rh}$: C 58.67, H 5.99, N 5.95; found: C 58.41, H 5.69, N 5.70.

General procedure for the synthesis of rhodium dicarbonyl derivatives: The respective [Rh(cod)] derivative was added to a dried Schlenk tube. The complex was backflashed three times with carbon monoxide and then dry CH_2Cl_2 was added (15 mL). The solution was stirred under a constant flux of CO for 30 min. The solution was concentrated in vacuum (≈ 5 mL) and precipitated by addition of *n*-hexane (≈ 30 mL) at 4°C.

Dicarbonylchlorido(1,3-dimethylbenzimidazol-2-ylidene)rhodium(I) (5a): Yield: 0.021 g (0.06 mmol, 48%) yellow powder. $^1\text{H NMR}$ (CDCl_3): δ = 4.14 (s, 6H, $-\text{NCH}_3$), 7.40 (m, 4H, ArH), $^{13}\text{C NMR}$ (CDCl_3): δ = 35.22 ($-\text{NCH}_3$), 110.40 and 123.69 (ArC), 134.85 (quaternary ArC), 182.40 (d, *cis*-CO, $^1J_{\text{RhC}} = 74.2$ Hz), 185.21, 185.30 (d, *trans*-CO, $^1J_{\text{RhC}} = 53.6$ Hz), 185.36 ppm (d, NHC, $^1J_{\text{RhC}} = 43.1$ Hz); FTIR: $\tilde{\nu}$ = 2074 ($\tilde{\nu}(\text{CO})_{\text{sym}}$), 1989 cm^{-1} ($\tilde{\nu}(\text{CO})_{\text{asym}}$); MS (EI): m/z : 318 [$\text{M}^+ - \text{CO}$]; elemental analysis calcd (%) for $\text{C}_{11}\text{H}_{10}\text{ClN}_2\text{O}_2\text{Rh}$: C 38.79, H 2.96, N 8.23; found: C 39.20, H 3.10, N 7.89.

Dicarbonylchlorido(1,3-diethylbenzimidazol-2-ylidene)rhodium(I) (5b): The preparation of this compound has been reported.^[52] Yield: 0.016 g (0.04 mmol, 33%) yellow powder. $^1\text{H NMR}$ (CDCl_3): δ = 1.58 (t, 6H, $^3J_{\text{K}} = 7.3$ Hz, $-\text{NCH}_2\text{CH}_3$), 4.62 (dq, 2H, $-\text{NCH}_2\text{CH}_3$, $^3J_{\text{HH}} = 7.3$ Hz, $^2J_{\text{HH}} = 14.4$ Hz), 4.75 (dq, 2H, $-\text{NCH}_2\text{CH}_3$, $^3J_{\text{HH}} = 7.3$ Hz, $^2J_{\text{HH}} = 14.4$ Hz), 7.36 (dd, 2H, ArH $_{4/7}$, $^4J_{\text{HH}} = 3.1$ Hz, $^3J_{\text{HH}} = 6.1$ Hz), 7.45 (dd, 2H, ArH $_{5/6}$, $^4J_{\text{HH}} = 3.1$ Hz, $^3J_{\text{HH}} = 6.1$ Hz); $^{13}\text{C NMR}$ (CDCl_3): δ = 14.79 ($-\text{NCH}_2\text{CH}_3$), 43.89 ($-\text{NCH}_2\text{CH}_3$), 110.77 and 123.47 (ArC), 134.02 (quaternary ArC), 182.61 (d, *cis*-CO, $^1J_{\text{RhC}} = 72.2$ Hz), 184.26 (d, NHC, $^1J_{\text{RhC}} = 42.5$ Hz), 185.30 ppm (d, *trans*-CO, $^1J_{\text{RhC}} = 53.8$ Hz); FTIR: 2077 ($\tilde{\nu}(\text{CO})_{\text{sym}}$), 1991 cm^{-1} ($\tilde{\nu}(\text{CO})_{\text{asym}}$); MS (EI): m/z : 340 [$\text{M}^+ - \text{CO}$]; elemental analysis calcd (%) for $\text{C}_{13}\text{H}_{14}\text{ClN}_2\text{O}_2\text{Rh}$: C 42.36, H 3.83, N 7.60; found: C 41.98, H 3.55, N 7.53.

Dicarbonylchlorido(1,3-diisopropylbenzimidazol-2-ylidene)rhodium(I) (5c): The preparation of this compound has previously been reported.^[53] Yield: 0.016 g (0.04 mmol, 37 %) yellow powder. ¹H NMR (CDCl₃): δ = 1.72 (dd, 12H, -NCH(CH₃)₂, ⁴J_{HH} = 1.4 Hz, ³J_{HH} = 7.0 Hz), 5.77 (hept, 2H, -NCH(CH₃)₂, ³J_{HH} = 7.0 Hz), 7.29 (dd, 2H, ArH_{4,7}, ⁴J_{HH} = 3.2 Hz, ³J_{HH} = 6.2 Hz), 7.62 (dd, 2H, ArH_{5,6}, ⁴J_{HH} = 3.2 Hz, ³J_{HH} = 6.2 Hz) ppm; ¹³C NMR (CDCl₃): δ = 20.91 and 21.19 (-NCH(CH₃)₂), 54.58 (-NCH(CH₃)₂), 112.97 and 122.84 (ArC), 133.41 (quaternary ArC), 182.58 (d, *cis*-CO, ¹J_{RhC} = 74.4 Hz), 182.89 (d, ArC², ¹J_{RhC} = 42.4 Hz), 185.52 ppm (d, *trans*-CO, ¹J_{RhC} = 53.7 Hz); FTIR: $\tilde{\nu}$ = 2086 (ν(CO)_{sym}), 1990 cm⁻¹ (ν(CO)_{asym}); MS (EI): 368 [M⁺-CO]; elemental analysis calcd (%) for C₁₅H₁₈ClN₂O₂Rh: C 45.42, H 4.57, N 7.06; found: C 45.37, H 4.49, N 6.88.

Dicarbonylchlorido(1,3-dibenzylbenzimidazol-2-ylidene)rhodium(I) (5d): Yield: 0.013 g (0.03 mmol, 28 %) yellow powder. ¹H NMR (CDCl₃): δ = 5.83 (d, 2H, -NCH₂Ar, ²J_{HH} = 15.7 Hz), 6.05 (d, 2H, -NCH₂Ar, ²J_{HH} = 15.7 Hz), 7.25–7.17 (m, 4H, ArH), 7.41–7.29 ppm (m, 10H, -NCH₂ArH); ¹³C NMR (CDCl₃): δ = 53.02 (-NCH₂Ar), 111.67, 123.78, 128.29, 128.98, 132.55, 135.05 (18C, ArC), 182.04 (d, *cis*-CO, ¹J_{RhC} = 74.2 Hz), 185.06 (d, *trans*-CO, ¹J_{RhC} = 53.8 Hz), 186.93 ppm (d, ArC², ¹J_{RhC} = 43.5 Hz). FTIR: $\tilde{\nu}$ = 2076 (ν(CO)_{sym}), 1994 cm⁻¹ (ν(CO)_{asym}); MS (EI): 464 [M⁺-CO]; elemental analysis calcd (%) for C₂₃H₁₈ClN₂O₂Rh: C 56.06 H 3.68 N 5.69; C 56.34, H 3.75, N 5.77.

Dicarbonylchlorido(1,3-diethylperimidin-2-ylidene)rhodium(I) (6): Yield: 0.012 g (0.03 mmol, 27 %) yellow powder. ¹H NMR (CDCl₃): δ = 1.51 (t, 6H, -NCH₂CH₃, ³J_{HH} = 7.1 Hz), 4.76 (m, 2H, -NCH₂CH₃), 5.03 (m, 2H, -NCH₂CH₃), 6.73 (dd, 2H, ArH, ⁴J_{HH} = 2.3 Hz, ³J_{HH} = 6.3 Hz), 7.40–7.34 ppm (m, 4H, ArH); ¹³C NMR (CDCl₃): δ = 11.06 (-NCH₂CH₃), 50.53 (-NCH₂CH₃), 105.80 (ArC), 121.41 (quaternary ArC), 121.86 and 127.79 (ArC), 133.20 and 135.00 (quaternary ArC), 182.43 (d, *cis*-CO, ¹J_{RhC} = 75.4 Hz), 185.56 (d, *trans*-CO, ¹J_{RhC} = 54.4 Hz), 199.29 ppm (d, NHC, ¹J_{RhC} = 41.3 Hz); FTIR: $\tilde{\nu}$ = 2079 (ν(CO)_{sym}), 2000 cm⁻¹ (ν(CO)_{asym}); MS (EI): 390 [M⁺-CO]; elemental analysis for calcd (%) for C₁₇H₁₆ClN₂O₂Rh: C 48.77 H 3.85 N 6.69; found: C 49.04, H 3.99, N 6.97.

Computational details: Relativistic density functional theory calculations^[73] were carried out by using the ADF 2012 code^[74] incorporating scalar corrections through the ZORA Hamiltonian.^[75,76] Triple-ξ Slater basis set plus two polarization functions (STO-TZ2P) for valence electrons were employed within the generalized gradient approximation (GGA) according to the Perdew–Burke–Ernzerhof (PBE) nonlocal exchange–correlation functional.^[77,78] The frozen core approximation was applied to the [1s²–3d¹⁰] core for Rh, and [1s²] for C, N, and Cl, leaving the remaining electrons to be treated variationally. Geometry optimizations were done without any symmetry restraint through the analytical energy gradient method implemented by Verluis and Ziegler.^[79] Bond-dissociation energies are corrected to the basis set superposition error (BSSE).

NMR properties were evaluated by employing the gauge-including atomic orbitals (GIAO) methodology^[80] as implemented in the NMR property module of the ADF code in conjunction to the GGA exchange expression proposed by Handy and Cohen^[81] and the correlation expression proposed by Perdew, Burke, and Ernzerhof (OPBE).^[77,78] The relative ¹³C NMR parameters (δ = σ_C^{TMS} – σ_C^{calcd}) were calculated by using the GIAO OPBE/ZORA level of theory and referenced to tetramethylsilane (TMS, σ_C^{TMS} = 191.19 ppm).

Antiproliferative effects in MCF-7 and HT-29 cells: The antiproliferative effects of the compounds were determined following an established procedure. In short, cells were suspended in cell culture medium (HT-29: 3000 cells mL⁻¹, MCF-7: 10000 cells mL⁻¹), and 100 μL aliquots thereof were plated in 96-well plates and incubated at 37 °C: 5% CO₂ for 48 h (HT-29) or 72 h (MCF-7). Stock solutions of the ruthenium complexes in DMF were freshly prepared and diluted with cell culture medium to the desired concentrations (final DMF concentration: 0.1% v/v). The medium in the plates was replaced with medium containing the compounds in graded concentrations (six replicates, 200 μL per well). After further incubation for 72 h (HT-29) or 96 h (MCF-7) the cell biomass was determined by crystal violet staining and the IC₅₀ values were determined as those concentrations causing 50% inhibition of cell proliferation. Results are represented as means of independent experiments.

TrxR inhibition assay: To determine the inhibition of TrxR, an established microplate reader-based assay was performed with minor modifications.^[16] For this purpose, commercially available rat recombinated TrxR1 (from IMCO Corporation) was used and diluted with distilled water to achieve a concentration of 0.01 U mL⁻¹. The compounds were freshly dissolved as stock solutions in DMF. Potassium phosphate buffer pH 7.0 (25 μL) containing the compounds in graded concentrations or vehicle (DMF) without compounds (control probe) were added to each aliquot of the enzyme solution (25 μL) and the resulting solutions (final concentration of DMF: 0.5% v/v) were incubated with moderate shaking for 75 min at 37 °C in a 96-well plate. The reaction mixture (225 of 1000 μL; the reaction mixture consisted of 500 μL potassium phosphate buffer pH 7.0, 80 μL 100 mM EDTA solution pH 7.5, 20 μL BSA solution 0.05%, 100 μL of 20 mM NADPH solution, and 300 μL of distilled water) was added to each well, and the reaction started by addition of an 20 mM ethanolic 5,5'-dithiobis(2-nitrobenzoic acid) solution (25 μL). After proper mixing, the formation of 5-thio-2-nitrobenzoic acid (5-TNB) was monitored with a microplate reader (PerkinElmer Victor X4) at 405 nm in 10 s intervals for 6 min. The increase in 5-TNB concentration over time followed a linear trend (r² ≥ 0.99), and the enzymatic activities were calculated as the slopes (increase in absorbance per second) thereof. For each tested compound, the noninterference with the assay components was confirmed by a negative control experiment by using an enzyme-free solution. The IC₅₀ values were calculated as the concentration of compound decreasing the enzymatic activity of the untreated control by 50% and are given as the means and error of repeated experiments.

Binding to albumin: Protein binding was studied according to a recently described method with minor modifications (see refs. [82] and [83]). Bovine serum albumin (BSA, 400 mg, Sigma Aldrich) was dissolved in Dulbecco's modified Eagle's medium (DMEM) high glucose (PAA) cell culture medium (10.0 mL) supplemented with gentamycin (50 mg L⁻¹). A stock solution (10 μL of 5.0 mM) of the correspondent complex in DMF was added to the BSA-treated medium and incubated at 37 °C in the dark under gentle shaking. After 0, 1, 2, 4, 6, 12, and 24 h, an aliquot (250 μL) thereof was taken, treated with of cold (–20 °C) ethanol (500 μL) and stored at –20 °C for 2 h to allow an optimal precipitation of the protein fraction. Afterwards the solution was centrifuged at 400 g for 5 min at 4 °C, an aliquot of the supernatant (400 μL) was taken and the rhodium content was measured by atomic absorption spectroscopy (AAS; see below). The results were expressed as percentage of rhodium bound to albumin and are given as the means and error of repeated experiments.

Binding to DNA: Experiments were performed according to a previously described method.^[69] Salmon testes DNA (Sigma) was dissolved in PBS pH 7.4 and the drugs were added as stock solutions in DMF. The final solutions contained **3a** (4.0 μM), salmon testes DNA (247.5 μg mL⁻¹) and 0.1% (v/v) DMF. After vortexing, the solutions were incubated at 37 °C for 2 h. Aliquots (200 μL) were mixed with 0.9 M sodium acetate (100 μL) and ice-cold ethanol (900 μL). Samples were stored at –20 °C for 30 min. The pellets were isolated by centrifugation (2390 g, 10 min, 4 °C) and re-suspended in 0.3 M sodium acetate (300 μL). Ice-cold ethanol (900 μL) was then added, and the precipitate was collected after centrifugation (2390 g, 10 min, 4 °C). Samples were washed twice with ice-cold ethanol and stored at –20 °C. The pellets were dissolved in water (500 μL, twice distilled), and the DNA content was determined by absorption reading at 260 nm in a microplate reader (PerkinElmer Victor X4). Salmon testes DNA dissolved in water were used for calibration purposes. The rhodium from the samples was determined by AAS. The amount of rhodium bound to DNA was expressed as percentage of total rhodium in the samples. Results were calculated as means of three independent experiments, which were performed with two replicates.

Uptake into the cells: For cellular-uptake studies HT-29 cells were grown until at least 70% confluency in 75 cm² cell culture flasks. Stock solutions of complex **3a** in DMF were freshly prepared and diluted with cell culture medium to the desired concentrations (final DMF concentration: 0.1% v/v, final complex concentration: 1.0 μM). The cell culture medium of the cell culture flasks was replaced with 10 mL of the cell culture medium (with or without bovine serum albumin (40 mg per mL)) solu-

tions containing **3a** and the flasks were incubated for 1, 4, and 6 h at 37°C/5% CO₂. Afterwards the medium was removed and the cells were washed with phosphate-buffered saline pH 7.4. After trypsinization, cell pellets were isolated by centrifugation, resuspended in 1–5 mL twice-distilled water, lysed by ultrasonication and appropriately diluted using twice-distilled water. The rhodium content of the samples was determined by AAS (see below) and the protein content of separate aliquots was determined by the Bradford method.

Uptake into the nuclei: The nuclei of HT-29 cells were isolated according to previously described procedure^[69,71] with some modifications: Cells were grown in 175 cm² cell culture flasks until at least 70% confluency. The cell culture medium was removed and replaced with cell culture medium (20 mL) containing 5 μM of **3a**. The flasks were incubated at 37°C/5% CO₂ for 1 and 6 h and the cell pellets were isolated as described above. After centrifugation (923 g, 5 min) the pellet was resuspended in 0.9% NaCl solution (1.0 mL) and an aliquot (200 μL) was removed before nuclei isolation to determine the total cellular rhodium uptake (see above). For nuclei isolation, the cell suspension was centrifuged at 923 g for 5 min and resuspended in 300 μL RSB-1 (0.01 M Tris-HCl, 0.01 M NaCl, 1.5 mM MgCl₂, pH 7.4) and left for 10 min in an ice bath. Swollen cells were centrifuged (1231 g, 5 min), resuspended in 300 μL of RSB-2 (RSB-1 containing each 0.3% v/v Nonidet-P40 and sodium desoxycholate) and homogenized by 10–15 up/down-pushes using a dounce homogenizer. The resultant homogenate was centrifuged at 3583 g for 5 min and the resulting crude nuclei were taken up in 0.25 M sucrose (150 μL) containing CaCl₂ (3 mM). The suspension was underlaid with 0.88 M sucrose (150 μL) and centrifuged for 10 min at 3583 g. The nuclei pellets were stored at –20°C or immediately dissolved in EDTA solution (200 μL of 10 g L⁻¹) and disrupted by ultrasonication. The rhodium content of the samples was determined by high-resolution continuum source atomic absorption spectrometry (HR-CS AAS, see below) and the nuclear protein content was determined by the Bradford method. Results are expressed as means of two independent experiments as pmol drug per mg nuclear protein. The ratio of drug taken up into the nucleus is calculated as percentage of the total rhodium content of each pellet.

AAS measurements: AAS measurements were performed using a contrAA 700 high-resolution continuum source atomic absorption spectrometer (HRCS-AAS) for the quantification of rhodium and platinum. Rhodium was detected at a wavelength of 343.4893 nm, whereas platinum was measured at 265.9450 nm. Standards for calibration purposes were prepared in a matrix-matched manner (in ethanol in case of albumin binding, in 100 μg mL⁻¹ aqueous DNA solution in case of DNA binding, and cellular matrix in case of cellular and nuclear uptake experiments, respectively) using a standard stock solution of **3a** or cisplatin. Triton X-100 (20 μL, 1%) and HNO₃ (20 μL, 13%) were added to each 200 μL sample or standard solution. A volume of 25 μL thereof was injected into the graphite tubes. Drying, pyrolysis, and atomization in the graphite furnace were performed according to the conditions previously reported for Rh^[40] and Pt^[84] with minor modifications. The mean absorbances of duplicate injections were used throughout the study.

Measurement of the mitochondrial membrane potential: Nalm-6 cells were incubated with different concentrations of complex **3a** for 48 h at 37°C and 5% CO₂. Afterwards, 1 mL of the cell suspension was centrifuged at 3000 rpm at 4°C for 5 min and the supernatant was removed carefully. JC-1 (6.25 μL, 0.2 mg mL⁻¹ in DMSO) was added to every sample and vortexed briefly. All samples were incubated for 30 min at 37°C, 300 rpm and vortexed briefly every 10 min. After incubation the samples were centrifuged at 4000 rpm, 4°C for 5 min. The supernatant was removed carefully and the pellet resuspended in PBS (200 μL) and analyzed using a FACScan (Becton Dickinson, Heidelberg, Germany) equipped with the CELLQuest software.

Measurement of DNA fragmentation: Apoptotic cell death was determined by a modified cell cycle analysis, which detects DNA fragmentation at the single-cell level. For measurement of DNA fragmentation, cells were seeded at a density of 1 × 10⁵ cells mL⁻¹ and treated with different concentrations of **3a**. After 72 h of incubation, cells were collected by centrifugation at 30 g for 5 min, washed with PBS at 4°C, and fixed in

PBS 2% (v/v) formaldehyde on ice for 30 min. After fixation, cells were incubated with ethanol/PBS (2:1, v/v) for 15 min, pelleted, and resuspended in PBS containing RNase A (40 μg mL⁻¹). After incubation for 30 min at 37°C, cells were pelleted again and finally resuspended in PBS containing propidium iodide (50 μg mL⁻¹). Nuclear DNA fragmentation was then quantified by flow cytometric determination of hypodiploid DNA. Data were collected and analyzed by using a FACScan (Becton Dickinson, Heidelberg, Germany) equipped with the CELLQuest software. Data are given in % hypoploidy (subG1), which reflects the number of apoptotic cells.

Acknowledgements

The financial support by DFG (grant to support the initiation of international collaboration), FONDECYT 11100027, FCI (Fonds der Chemischen Industrie), Dr. Kleist-Foundation, Berlin, Dr. Koch-Foundation, Berlin, as well as the excellent technical support by Davida Fernandez Fernandez are gratefully acknowledged.

- [1] G. Gasser, I. Ott, N. Metzler-Nolte, *J. Med. Chem.* **2011**, *54*, 3–25.
- [2] M. Patra, G. Gasser, *ChemBioChem* **2012**, *13*, 1232–1252.
- [3] C. G. Hartinger, N. Metzler-Nolte, P. J. Dyson, *Organometallics* **2012**, *31*, 5677–5685.
- [4] A. L. Noffke, A. Habtemariam, A. M. Pizarro, P. J. Sadler, *Chem. Commun.* **2012**, *48*, 5219–5246.
- [5] L. Oehninger, R. Rubbiani, I. Ott, *Dalton Trans.* **2013**, *42*, 3269–3284.
- [6] W. Liu, R. Gust, *Chem. Soc. Rev.* **2013**, *42*, 755–773.
- [7] A. Gautier, F. Cisnetti, *Metallomics* **2012**, *4*, 23–32.
- [8] A. Kascatan-Nebioglu, M. J. Panzner, C. A. Tessier, C. L. Cannon, W. J. Youngs, *Coord. Chem. Rev.* **2007**, *251*, 884–895.
- [9] F. Hackenberg, G. Lally, H. Müller-Bunz, F. Paradisi, D. Quaglia, W. Streciwilk, M. Tacke, *Inorg. Chim. Acta* **2013**, *395*, 135–144.
- [10] S. Patil, K. Dietrich, A. Deally, B. Gleeson, H. Müller-Bunz, F. Paradisi, M. Tacke, *Helv. Chim. Acta* **2010**, *93*, 2347–2364.
- [11] J. G. Leid, A. J. Ditto, A. Knapp, P. N. Shah, B. D. Wright, R. Blust, L. Christensen, C. B. Clemons, J. P. Wilber, G. W. Young, A. G. Kang, M. J. Panzner, C. L. Cannon, Y. H. Yun, W. J. Youngs, N. M. Seckinger, E. K. Cope, *J. Antimicrob. Chemother.* **2012**, *67*, 138–148.
- [12] J. L. Hickey, R. A. Ruhayel, P. J. Barnard, M. V. Baker, S. J. Berners-Price, A. Filipovska, *J. Am. Chem. Soc.* **2008**, *130*, 12570–12571.
- [13] S. J. Berners-Price, A. Filipovska, *Metallomics* **2011**, *3*, 863–873.
- [14] R. Rubbiani, S. Can, I. Kitanovic, H. Alborzina, M. Stefanopoulou, M. Kokoschka, S. Mönchgesang, W. S. Sheldrick, S. Wölfl, I. Ott, *J. Med. Chem.* **2011**, *54*, 8646–8657.
- [15] E. Schuh, C. Pflüger, A. Citta, A. Folda, M. P. Rigobello, A. Bindoli, A. Casini, F. Mohr, *J. Med. Chem.* **2012**, *55*, 5518–5528.
- [16] R. Rubbiani, I. Kitanovic, H. Alborzina, S. Can, A. Kitanovic, L. A. Onambe, M. Stefanopoulou, Y. Geldmacher, W. S. Sheldrick, G. Wolber, A. Prokop, S. Wölfl, I. Ott, *J. Med. Chem.* **2010**, *53*, 8608–8618.
- [17] R. Rubbiani, E. Schuh, A. Meyer, J. Lemke, J. Wimberg, N. Metzler-Nolte, F. Meyer, F. Mohr, I. Ott, *MedChemComm* **2013**, *4*, 942–948.
- [18] O. Rackham, A.-M. J. Shearwood, R. Thyer, E. McNamara, S. M. K. Davies, B. A. Callus, A. Miranda-Vizuete, S. J. Berners-Price, Q. Cheng, E. S. J. Arnér, A. Filipovska, *Free Radical Biol. Med.* **2011**, *50*, 689–699.
- [19] M. Baker, P. J. Barnard, S. J. Berners-Price, S. K. Brayshaw, J. L. Hickey, B. W. Skelton, A. H. White, *Dalton Trans.* **2006**, 3708–3715.
- [20] M. Skander, P. Retailleau, B. Bourrie, L. Schio, P. Mailliet, A. Marinetti, *J. Med. Chem.* **2010**, *53*, 2146–2154.
- [21] S. D. Adhikary, D. Bose, P. Mitra, K. D. Saha, V. Bertolasi, J. Dinda, *New J. Chem.* **2012**, *36*, 759–767.

- [22] R. Wai-Yin Sun, A. Lok-Fung Chow, X.-H. Li, J. J. Yan, S. Sin-Yin Chui, C.-M. Che, *Chem. Sci.* **2011**, *2*, 728–736.
- [23] G. Alves, L. Morel, M. El-Ghozzi, D. Avignat, B. Legeret, L. Nauton, F. Cisnetti, A. Gautier, *Chem. Commun.* **2011**, *47*, 7830–7832.
- [24] T. Zou, C.-N. Lok, Y. M. E. Fung, C.-M. Che, *Chem. Commun.* **2013**, *49*, 5423–5425.
- [25] C.-H. Wang, W.-C. Shih, H. C. Chang, Y.-Y. Kuo, W.-C. Hung, T.-G. Ong, W.-S. Li, *J. Med. Chem.* **2011**, *54*, 5245–5249.
- [26] S. Ray, R. Mohan, J. K. Singh, M. K. Samantaray, M. M. Shaikh, D. Panda, P. Ghosh, *J. Am. Chem. Soc.* **2007**, *129*, 15042–15053.
- [27] O. Ciftci, A. Beytur, N. Vardi, I. Ozdemir, *Drug Dev. Ind. Pharm.* **2012**, *38*, 40–46.
- [28] L. Oehninger, M. Stefanopoulou, H. Alborzina, J. Schur, S. Ludewig, K. Namikawa, A. Muñoz-Castro, R. W. Köster, K. Baumann, S. Wölfl, W. S. Sheldrick, I. Ott, *Dalton Trans.* **2013**, *42*, 1657–1666.
- [29] L. Oehninger, H. Alborzina, S. Ludewig, K. Baumann, S. Wölfl, I. Ott, *ChemMedChem* **2011**, *6*, 2142–2145.
- [30] B. Cetinkaya, E. Cetinkaya, H. Kucubay, R. Durmaz, *Arzneim.-Forsch./Drug Res.* **1996**, *46*, 821–823.
- [31] J. R. McConnell, D. P. Rananaware, D. M. Ramsey, K. N. Buys, M. L. Cole, S. R. McAlpine, *Bioorg. Med. Chem. Lett.* **2013**, *23*, 2527–2531.
- [32] M. A. Scharwitz, I. Ott, Y. Geldmacher, R. Gust, W. S. Sheldrick, *J. Organomet. Chem.* **2008**, *693*, 2299–2309.
- [33] M. Harlos, I. Ott, R. Gust, H. Alborzina, S. Wölfl, A. Kromm, W. S. Sheldrick, *J. Med. Chem.* **2008**, *51*, 3924–3933.
- [34] Y. Geldmacher, I. Kitanovic, H. Alborzina, K. Bergerhoff, R. Rubbiani, P. Wefelmeier, A. Prokop, R. Gust, I. Ott, S. Wölfl, W. S. Sheldrick, *ChemMedChem* **2011**, *6*, 429–439.
- [35] M. Dobroschke, Y. Geldmacher, I. Ott, M. Harlos, L. Kater, L. Wagner, R. Gust, W. S. Sheldrick, A. Prokop, *ChemMedChem* **2009**, *4*, 177–187.
- [36] Y. Geldmacher, M. Oleszak, W. S. Sheldrick, *Inorg. Chim. Acta* **2012**, *393*, 84–102.
- [37] M. B. Schwarz, A. Kurzwernhart, A. Roller, W. Kandoller, B. K. Keppler, C. G. Hartinger, *Z. Anorg. Allg. Chem.* **2013**, 1648–1654.
- [38] R. Payne, P. Govender, B. Therrien, C. M. Clavel, P. J. Dyson, G. S. Smith, *J. Organomet. Chem.* **2013**, *729*, 20–27.
- [39] R. J. Ernst, A. C. Komor, J. K. Barton, *Biochemistry* **2011**, *50*, 10919–10928.
- [40] F. Hackenberg, L. Oehninger, H. Alborzina, S. Can, I. Kitanovic, Y. Geldmacher, M. Kokoschka, S. Wölfl, I. Ott, W. S. Sheldrick, *J. Inorg. Biochem.* **2011**, *105*, 991–999.
- [41] G. Sava, T. Giraldo, G. Mestroni, G. Zassinovich, *Chem.-Biol. Interact.* **1983**, *45*, 1–6.
- [42] Y. Li, C. d. Kock, P. J. Smith, H. Guzgay, D. T. Hendricks, K. Naran, V. Mizrahi, D. F. Warner, K. Chibale, G. S. Smith, *Organometallics* **2013**, *32*, 141–150.
- [43] U. Sliwinska-Hill, F. P. Pruchnik, M. Latocha, D. Nawrocka-Musial, S. Ułaszewski, *Inorg. Chim. Acta* **2013**, *400*, 26–31.
- [44] G. Rubner, K. Bendorf, A. Wellner, S. Bergemann, I. Ott, R. Gust, *Eur. J. Med. Chem.* **2010**, *45*, 5157–5163.
- [45] S. Patil, A. Deally, B. Gleeson, H. Müller-Bunz, F. Paradisi, M. Tacke, *Metallomics* **2011**, *3*, 74–88.
- [46] I. Özdemir, N. Temelli, S. Günel, S. Demir, *Molecules* **2010**, *15*, 2203–2210.
- [47] S. Patil, A. Deally, F. Hackenberg, L. Kaps, H. Müller-Bunz, R. Schobert, M. Tacke, *Helv. Chim. Acta* **2011**, *94*, 1551–1562.
- [48] S. Patil, A. Deally, B. Gleeson, F. Hackenberg, H. Müller-Bunz, F. Paradisi, M. Tacke, *Z. Anorg. Allg. Chem.* **2011**, *637*, 386–396.
- [49] J. M. Herbert, P. D. Woodgate, W. A. Denny, *J. Med. Chem.* **1987**, *30*, 2081–2086.
- [50] E. Çetinkaya, P. B. Hitchcock, H. Küçükbay, M. F. Lappert, S. Al-Juaid, *J. Organomet. Chem.* **1994**, *481*, 89–95.
- [51] F. E. Hahn, T. von Fehren, L. Wittenbecher, R. Fröhlich, *Z. Naturforsch.* **2004**, *59b*, 541–543.
- [52] J. A. V. Er, A. G. Tennyson, J. W. Kamplain, V. M. Lynch, C. W. Bielawski, *Eur. J. Inorg. Chem.* **2009**, 1729–1738.
- [53] B. Hildebrandt, S. Raub, W. Frank, C. Ganter, *Chem. Eur. J.* **2012**, *18*, 6670–6678.
- [54] C. A. Tolman, *Chem. Rev.* **1977**, *77*, 313–348.
- [55] W. A. Herrmann, J. Schütz, G. D. Frey, E. Herdtweck, *Organometallics* **2006**, *25*, 2437–2448.
- [56] K. Nakamoto, *Infrared and Raman Spectra of Inorganic and Coordination Compounds, Applications in Coordination, Organometallic, and Bioinorganic Chemistry*, Wiley-VCH, Weinheim, **2009**.
- [57] P. S. Pregosin, *NMR in Organometallic Chemistry*, Wiley-VCH, Weinheim, **2012**.
- [58] A. Bittermann, E. Herdtweck, P. Härter, W. A. Herrmann, *Organometallics* **2009**, *28*, 6963–6968.
- [59] F. M. Bickelhaupt, E. J. Baerends, K. B. Lipkowitz, D. B. Boyd, *Reviews in Computational Chemistry*, Wiley-VCH, Weinheim, **2005**.
- [60] M. Pellei, V. Gandin, M. Marinelli, C. Marzano, M. Yousufuddin, H. V. R. Dias, C. Santini, *Inorg. Chem.* **2012**, *51*, 9873–9882.
- [61] P. Mura, M. Camalli, A. Bindoli, F. Sorrentino, A. Casini, C. Gabbiani, M. Corsini, P. Zanello, M. P. Rigobello, L. Messori, *J. Med. Chem.* **2007**, *50*, 5871–5874.
- [62] A. Casini, C. Gabbiani, F. Sorrentino, M. P. Rigobello, A. Bindoli, T. J. Geldbach, A. Marrone, N. Re, C. G. Hartinger, P. J. Dyson, L. Messori, *J. Med. Chem.* **2008**, *51*, 6773–6781.
- [63] A.-B. Witte, K. Anestäl, E. Jerremalm, H. Ehrsson, E. S. J. Arner, *Free Radical Biol. Med.* **2005**, *39*, 696–703.
- [64] W. Cai, L. Zhang, Y. Song, B. Wang, B. Zhang, X. Cui, G. Hu, Y. Liu, J. Wu, J. Fang, *Free Radical Biol. Med.* **2012**, *52*, 257–265.
- [65] A. Bindoli, M. P. Rigobello, G. Scutari, C. Gabbiani, A. Casini, L. Messori, *Coord. Chem. Rev.* **2009**, *253*, 1692–1707.
- [66] C. Gabbiani, G. Mastrobuoni, F. Sorrentino, B. Dani, M. P. Rigobello, A. Bindoli, M. A. Cinellu, G. Pieraccini, L. Messoria, A. Casini, *MedChemComm* **2011**, *2*, 50–54.
- [67] J. Lu, E.-H. Chew, A. Holmgren, *Proc. Natl. Acad. Sci. USA* **2007**, *104*, 12288–12293.
- [68] K. N. de Oliveira, V. Andermark, S. von Grafenstein, L. A. Onambele, G. Dahl, R. Rubbiani, G. Wolber, C. Gabbiani, L. Messori, A. Prokop, I. Ott, *ChemMedChem* **2013**, *8*, 256–264.
- [69] J. Schur, C. M. Manna, A. Deally, R. W. Köster, M. Tacke, E. Y. Tshuva, I. Ott, *Chem. Commun.* **2013**, *49*, 4785–4787.
- [70] M. Groessel, O. Zava, P. J. Dyson, *Metallomics* **2011**, *3*, 591–599.
- [71] I. Ott, K. Schmidt, B. Kircher, P. Schumacher, T. Wiglenda, R. Gust, *J. Med. Chem.* **2005**, *48*, 622–629.
- [72] A. G. Weidmann, A. C. Komor, J. K. Barton, *Philos. Trans. R. Soc. A* **1995**, *371*, 20120117.
- [73] G. Lümmen, H. Sperling, H. Luboldt, T. Otto, H. Rübber, *Cancer Chemother. Pharmacol.* **1998**, *42*, 415–417.
- [74] Amsterdam Density Functional (ADF), Vrije Universiteit, Amsterdam (The Netherlands), **2012**.
- [75] E. van Lenthe, E. J. Baerends, J. G. Snijders, *J. Chem. Phys.* **1994**, *101*, 9783–9792.
- [76] K. G. Dyall, K. Fægri, *Introduction to Relativistic Quantum Chemistry*, Oxford University Press, Oxford, New York, **2007**.
- [77] J. P. Perdew, K. Burke, Y. Wang, *Phys. Rev. B* **1996**, *54*, 16533–16539.
- [78] J. P. Perdew, K. Burke, M. Ernzerhof, *Phys. Rev. Lett.* **1996**, *77*, 3865–3868.
- [79] L. Versluis, T. Ziegler, *J. Chem. Phys.* **1988**, *88*, 322–328.
- [80] K. Wolinski, J. F. Hinton, P. Pulay, *J. Am. Chem. Soc.* **1990**, *112*, 8251–8260.
- [81] N. C. Handy, A. J. Cohen, *Mol. Phys.* **2001**, *99*, 403–412.
- [82] I. Ott, R. Gust, *Biometals* **2005**, *18*, 171–177.
- [83] J. Ma, G. Stoter, J. Verweij, J. H. M. Schellens, *Cancer Chemother. Pharmacol.* **1996**, *38*, 391–394.
- [84] R. Gust, B. Schnurr, R. Krauser, G. Bernhardt, M. Koch, B. Schmid, E. Hummel, H. Schönenberger, *J. Cancer Res. Clin. Oncol.* **1998**, *124*, 585–597.

Received: July 18, 2013

Revised: September 17, 2013

Published online: November 15, 2013